JOURNAL OF CATALYSIS **177,** 129–136 (1998)
ARTICLE NO. CA982063

Catalytic Properties of Pd Deposited on SiC(0001) Single Crystal Surfaces

L. Lianos, A. Berthet, C. Deranlot, F. J. Cadete Santos Aires, J. Massardier, and J. C. Bertolini[1]

Institut de Recherches sur la Catalyse, conventionné à l'UCB-Lyon1, 2 avenue Albert Einstein, F-69626 Villeurbanne Cedex, France

Received November 4, 1997; revised February 6, 1998; accepted February 11, 1998

The catalytic properties of Pd deposited on SiC(0001) single crystals were examined. The SiC surface was prepared by ion bombardment and annealing, and characterised by AES, LEED, and XPS under UHV conditions. The surfaces obtained showed a carbon terminated surface, with a (1 × 1) LEED pattern. The model catalyst was obtained by vapodeposition of pure Pd. Three deposits were particularly studied corresponding respectively to 1.9×10^{14}, 5.4×10^{14}, and 2.9×10^{15} Pd/cm^2. The Pd/SiC deposits were first characterised by AES, XPS, and tapping mode AFM. From quantitative treatment of the XPS data and analysis of AFM images (obtained "in air" on these surfaces after a reaction) one concludes that Pd particles are rather "flat." Moreover, Pd particles were found to retain some interaction with the SiC support leading to nearly a 1-eV higher energy of the $Pd_{3d5/2}$ level measured by XPS, as compared to massic Pd. Their catalytic properties were tested for the 1,3-butadiene hydrogenation reaction. The activities obtained, per Pd surface atom, range above those found for Pd surface atoms on pure Pd(111) and Pd(110).

Key Words: **catalysis; palladium; vapodeposition; silicon carbide; single crystals; reactivity; 1-3 butadiene.**

INTRODUCTION

Refractory materials having good thermal conductivity, such as SiC, display a potential interest as supports for metallic catalysts. Indeed, they are expected to be very stable at high temperature and for largely exothermic reactions exhibiting high turnover frequencies (TOF) because of the high thermal conductivity of SiC, which could avoid the sintering of the metallic active phase. Recent works have indeed shown that employing such catalysts can be very successful in exothermic reactions (1–4). However, only little information about the metal/SiC close interaction on such catalysts is available (3, 5). The nucleation and the growth mechanism of the deposited metallic active phase must be influenced by the surface composition and structure of SiC. So, in order to go further on, studies of the growth mechanism of active metals on different kinds of SiC surfaces, Si terminated and/or C terminated, for instance, and the consequences on the catalytic performances (activity and selectivity) of such model catalysts for reactions testing the intrinsic properties of the metallic phase (hydrogenation and oxidation reactions) have to be carried out.

In the present work we studied the Pd layered, by atomic beam deposition technique, on a SiC(0001) single crystal substrate. The test reaction of the chemical properties of the active metallic phase was the hydrogenation of 1,3-butadiene, a reaction for which Pd is the most commonly used catalyst. The surface characterisation was done by *in-situ* auger electron spectroscopy (AES), low electron energy diffraction (LEED), quasi *in situ* X-ray photoelectron spectroscopy (XPS), and "in-air" tapping mode atomic force microscopy (TM-AFM).

EXPERIMENTAL

The SiC single crystal samples were obtained from CREE (NC, USA). They presented the hexagonal 6H type structure.

The experimental setting has been fully described elsewhere (6). It combines the following parts:

i. a UHV chamber (base pressure of 5×10^{-10} mbar), where clean surfaces were obtained by repeated cycles of Ar^+ ion bombardment (3.5 keV energy) and heating with an IR lamp. A four-grid LEED and AES (retarding field analyser) facilities were also available in order to control *in situ* the surface before and after reaction.

ii. a preparation chamber (base pressure of 3×10^{-9} mbar) equipped with Knudsen cells for metal evaporation. The Pd deposition rate was 2.4×10^{13} cm^{-2} s^{-1}. It was controlled by a quartz microbalance, which was formerly calibrated by measuring the deposited quantities by Rutherford backscattering spectroscopy. In all cases the Pd on SiC deposits were prepared under UHV conditions. The Pd deposition was made on a limited area of the sample, 0.65 cm^2, corresponding to a circular diaphragm of 0.9 cm diameter located just in front of the SiC support.

[1] To whom correspondence should be addressed. E-mail: bertol@catalyse.univ-lyon1.fr.

0021-9517/98 $25.00

iii. a low volume (84 cm^3) reactor in which the sample can be isolated after transfer under UHV conditions, that is capable of working at pressures higher than the atmospheric pressure. It operates in the static mode. It has been slightly modified in order to make the sampling for chromatography analysis possible.

The progress of the reaction was firstly monitored by means of a mass spectrometer located in the preparation chamber communicating through a leak valve with the reactor. In a second experiment, the reaction gases were introduced, through a valve, into a smaller volume (<3 cm^3) in which a septum was adjusted. A gas sample could thus be taken several times during a reaction run by means of a syringe (1 ml) through the septum and then analysed by gas phase chromatography. Care was taken to limit the number of samplings so that the reaction rate was not perturbed by the modification of the partial pressures and by the possible introduction of some air through the nipple.

iv. a UHV box, pumped separately by a 20 liter/s ion pump, allowing transfer of samples without exposure to air to the XPS instrument.

XPS was carried out in an ESCALAB 200R (Fisons Inst., UK), with using an Al Kα line. The C_{1s} and Si_{2p} peak decomposition was done using a multidimensional nonlinear optimisation method (7). The FWHM was set to 1.7 eV for the C_{1s} peak and 2.0 eV for the Si_{2p} peak and the Gauss–Lorentz mixing parameter was set to 0.7/0.3. The centre energy and the height of the peaks were determined by the multidimensional nonlinear optimisation method.

AFM observations were performed in air with a Nanoscope III Multimode (Digital Instruments Inc., Santa Barbara, CA, USA). Since the particles are supposed to be weakly bounded to the SiC surface the use of contact AFM is not very suitable as the particles will most certainly be swept aside by the rastering of the tip over the surface. We have thus used a more suitable imaging mode which is tapping mode AFM (TM-AFM) where the tip oscillates at high frequency (around 300 kHz) and comes into contact with the surface at each oscillation (it "taps" the surface). As the tip is scanned over the surface one can record the modification induced by the surface height variation to the oscillation amplitude obtaining thus a topographic image of the surface (8). Since the tip is not in permanent contact with the surface during the scan, sample deterioration is minimised. Si tips with typical curvature radius of 10 nm were used.

RESULTS AND DISCUSSION

We will first present the results relative to the cleaning and characterisation procedure of the SiC support itself. Afterwards, the behaviour of the Pd/SiC deposits will be described.

(a) The SiC(0001) Support

The SiC support preparation was standardised to repeated cycles of Ar^+ ion bombardment (3.5 keV energy) followed by a short annealing (5 min) at 870 K.

In Fig. 1 are reported the C_{1s} and Si_{2p} XPS spectra of a so-treated SiC(0001) sample, for two angles (90° and 30°, respectively with respect to the surface plane). The Si_{2p} photoelectric peak is largely dominated by a component attributed to Si bonded to C which is used as the reference peak and is set to 100.2 eV. Values found in the literature for the energy of the Si_{2p} peak for Si bonded with C in SiC vary from 100.0 to 100.6 eV (9–12). Some contribution of SiO_x species is also detected near 102 eV energy. The C_{1s} peak can be decomposed into three contributions. The main one, appearing at 282.7 eV, is attributed to the carbide SiC form. The second one, located near 284.2 eV, whose intensity increased when the measurement was made nearer grazing emergence for the photoelectrons, has to be associated to the presence of some excess of carbon at the surface. It can be attributed to some graphite formation by the excess of carbon present in the surface region, as frequently postulated (13, 14), or to some special form of carbon terminating the SiC(0001) surface (15). From the quantitative XPS data a simple "layer by layer" model (with attenuation of the

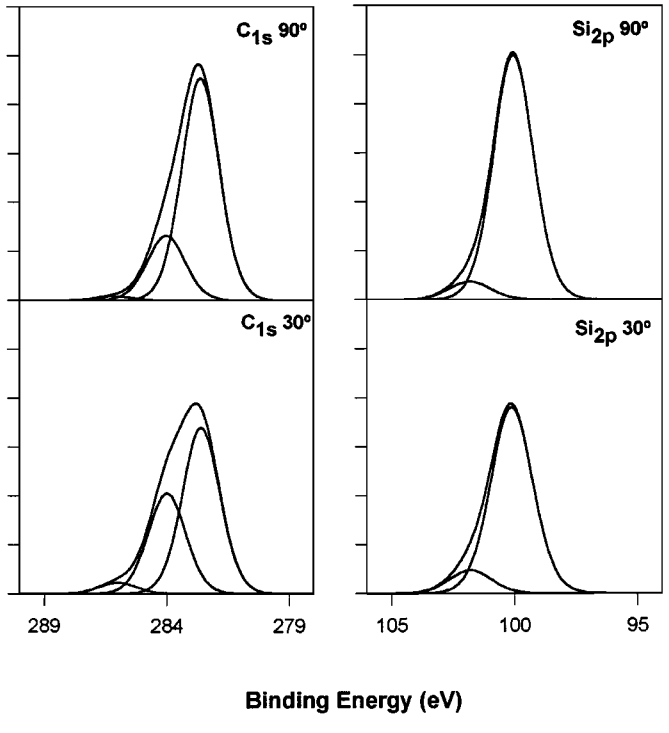

FIG. 1. C_{1s} and Si_{2p} XPS spectra obtained on the SiC(0001) sample after Ar^+ ion bombardment (3.5 keV energy) and further annealing (870 K). The spectra are presented here after background substraction and decomposition. The results are given for two exit angles (90° and 30° with respect to the surface plane), and an $Al_{K\alpha}$ X-ray source.

TABLE 1

Si and C Concentration Ratios Deduced from the Si_{2p} and C_{1s} XPS Peaks Obtained on the SiC(0001) Given in Fig. 1, after Data Treatments (Background Subtraction and Decomposition)

	Sputtered		Annealed	
	90°	30°	90°	30°
C(SiC)/Si(SiC)	0.68	0.68	0.74	0.74
C(284.2 eV)/C(SiC)	0.39	0.67	0.32	0.59

intensity of the photoelectrons in the material following a classical Lambert–Beer law) allows us to estimate the thickness of the C surface layer to about one/two atomic layers. Finally, the very small C_{1s} peak (at ≈286 eV) corresponds to some CO like "contamination" carbon.

The LEED pattern observed on the Ar^+ ion (3.5 keV, 0.5 $\mu A \cdot cm^{-2}$, 10 min) sputtered and annealed (at 870 K) surface corresponds to a (1×1) structure.

It has to be noted that the 1–2 layers of carbon terminating the structure were present at the extreme surface even just after ion bombardment. The short annealing we used did not actually affect that C component; it only structures the surface, as evidenced by the appearance of spots on the LEED pattern. Consequently, The surface can be regarded as a 1–2 C epitaxial layer(s) on a SiC substrate having characteristics a bit different than graphite, as demonstrated by the results using the synchrotron radiation facilities (15). In any case, one has to anneal at higher temperatures (around 1400 K) to get a surface with an higher carbon content; this carbon has then the characteristics of graphite (13–15). The results are summarised in Table 1.

The C/Si stoichiometry determined from the C and Si XPS peaks components (associated to SiC) is not found to equal one. It seems to be characteristic of some excess of Si, i.e. of some lack of C, in the SiC structure just under the outer C-rich surface. However, some uncertainty could come from an underestimation of the C(SiC) contribution in the C_{1s} peak during the decomposition.

The Pd deposits have been made on the SiC(0001) sample, used as support, prepared by sputtering and a short annealing at 870 K, which present a well-organised C-terminated surface.

(b) The Pd Deposits

Three Pd deposits were investigated. Two submonolayer ones containing approximately 1.9×10^{14} (sample #1) and 5.4×10^{14} Pd atoms/cm^2 (sample #2), and a "multi" layer one containing 2.9×10^{15} Pd atoms/cm^2 (sample #3).

XPS Measurements

The XPS measurements were made directly after deposition and prior to reaction. Pd_{3d}, C_{1s} and Si_{2p} XPS peaks are given in Fig. 2 for the three Pd deposits on SiC(0001) and for an exit angle of the photoelectrons at 90° with respect to the surface plane. The results of the treatment of the raw data for the three samples and for both 90° and 30–40° exit angles are reported in Table 2. The XPS peak located near 284.2 eV can be regarded as the contribution of two components: the outer 1–2 monolayer of carbon evidenced on the SiC crystal and some carbon pollution which can vary, depending on the time necessary for the complex transfer of samples from the elaboration cell to the analysis chamber. This contribution seems to be larger when the Pd content is higher.

The energy of the Pd_{3d} is very similar for the three deposits going from 336.0–336.1 for the 2 ML Pd sample to 336.2–336.3 for the submonolayer ones; only the shape of the peaks undergoes small changes (Fig. 2). The energy value (336.0 to 336.3 eV), is slightly higher than that measured for a pure Pd sample, 335.4 eV. Given the imprecision of the reference energy used we tried to estimate the value for "metallic" Pd by preparing another sample, where 9.07×10^{15} atoms/cm^2 of Pd were deposited (∼6 equivalent Pd layers); the energy of the Pd_{3d} peak was measured at 335.7 eV. There is only a small increase in the value of the $Pd_{3d5/2}$ photoelectric peak energy with decreasing Pd coverage on the SiC(0001) substrate. This is quite different from what is observed generally. Indeed, on many other substrates, such as silica, alumina, amorphous carbon, graphite, a significant upward shift of the Pd $3d_{5/2}$ photoelectric peak has been measured for low Pd content attributed to the presence of very small Pd particles (16–18), i.e. lower than 2–3 nm in diameter, or very flat (6), i.e. of less than 2–3 atomic layers thickness. One can therefore *a priori* think either that the particles remain very small while increasing the Pd coverage, even for the two monolayer #3 sample, or that some interaction is retained between Pd particles and the considered SiC support, even if a 3D-like growth exists.

Let us now consider the relative areas of the Pd_{3d} and Si_{2p} photoelectron peaks. Assuming a layer by layer growing mode and a classical model with attenuation of the intensity of the photoelectrons in the material following a classical Lambert–Beer law, the thickness of the Pd layer is calculated to be respectively 0.1, 0.5, and 2 monolayers (ML) for the considered samples, with 1 ML $= 1.53 \times 10^{15}$ Pd/cm^2 which corresponds to the surface density for the Pd(111) face. These values fit well the effective amount of deposited Pd both at 30° (40° for the #1 sample), and 90° for the exit angle of the photoelectrons with respect to the surface. This indicates that Pd is well dispersed on the SiC surface, on both samples. With respect to such results, one can think that the ad-layer grows either in a 2D configuration or forms very small aggregates.

In order to go further in the characterisation of the Pd ad-layer TM-AFM was used.

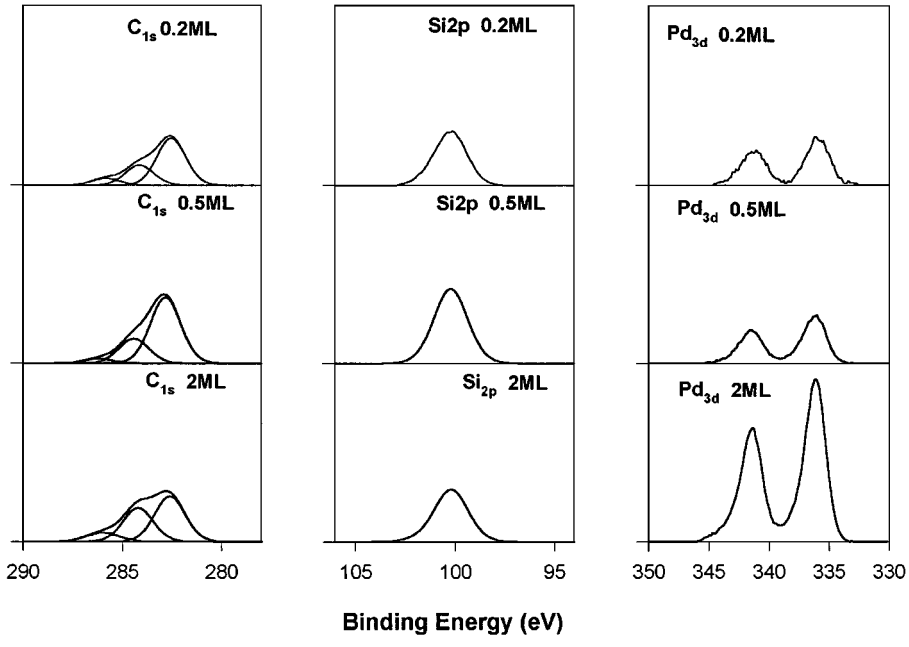

FIG. 2. XPS spectra (with arbitrary units for the Y-axis) of Pd_{3d}, C_{1s}, and Si_{2p} for respectively 1.9×10^{14}, 5.4×10^{14}, and 2.9×10^{15} Pd/cm^2 deposits on SiC(0001), after background substraction and decomposition. The results are given for an exit angle of 90° with respect to the surface plane and an AlKα X-ray source.

Atomic Force Microscopy Observations

Images obtained by TM-AFM show a very flat surface in the case of the single crystal (Fig. 3a); only some traces of polishing can be observed. In areas of up to 5 μm maximum height variations of about 7 nm (peak-to-valley) are observed and the mean roughness (R_a) is around 0.8 nm.

In the case of samples #1 (Fig. 3b), #2 (Fig. 3c), and #3 the images show randomly distributed particles. The image presented here of samples #1 and #2 were acquired after reaction, but images acquired before reaction are very similar.

From a quantitative point of view the direct measurement of particle size in the AFM images is not very accurate since the obtained images are the result of an addition of geometric contributions of tip and sample. However, in the case of sample #1 an estimation of the particle size can be obtained, assuming typical characteristics of the tip (namely a curvature radius of the tip of 10 nm and hemispheric apex ending a conical tip). The particles have apparent (AFM) sizes (Table 3) of about 20 nm which correspond, after taking into account tip contribution (in this method we need to use badly known parameters, such as the precise tip curvature radius, to deduce the size of the particles), to particle real sizes of about 10 nm; the measured heights of the particles are around 2 nm. By taking into account the density of particles, together with the mean diameter (see Table 3), one can estimate the surface fraction covered by palladium as around 3%. A simple calculation allows us to estimate heights of seven nearby atomic layers for the Pd particles of the 0.2 ML deposit, assuming an interatomic distance of 0.225 nm (the value for (111) palladium planes) between successive Pd planes. Such a value is not very far from that

TABLE 2

$Pd_{3d5/2}$ Binding Energy Value (eV) Together with Pd, Si, and C Concentration Ratios Deduced from the Pd_{3d}, Si_{2p}, and C_{1s} XPS Peaks of the Pd-SiC(0001) Deposits Given in Fig. 2, after Data Treatment (Background Subtraction and Decomposition)

	#1 (1.9 10^{14} at/cm^2)		#2 (5.4 10^{14} at/cm^2)		#3 (2.9 10^{15} at/cm^2)	
	90°	40°	90°	30°	90°	30°
$Pd_{3d5/2}$	336.2	336.3	336.1	336.1	336.1	336.0
C(SiC)/Si(SiC)	0.68	0.66	0.71	0.71	0.70	0.70
C(284.2 eV)/C(SiC)	0.42	0.93	0.39	0.96	0.77	1.74
$Pd_{3d5/2}$/Si(SiC)	0.01	0.016	0.08	0.14	0.37	0.71

Note. The energy of the Si_{2p} peak of SiC is taken as reference at 100.2 eV.

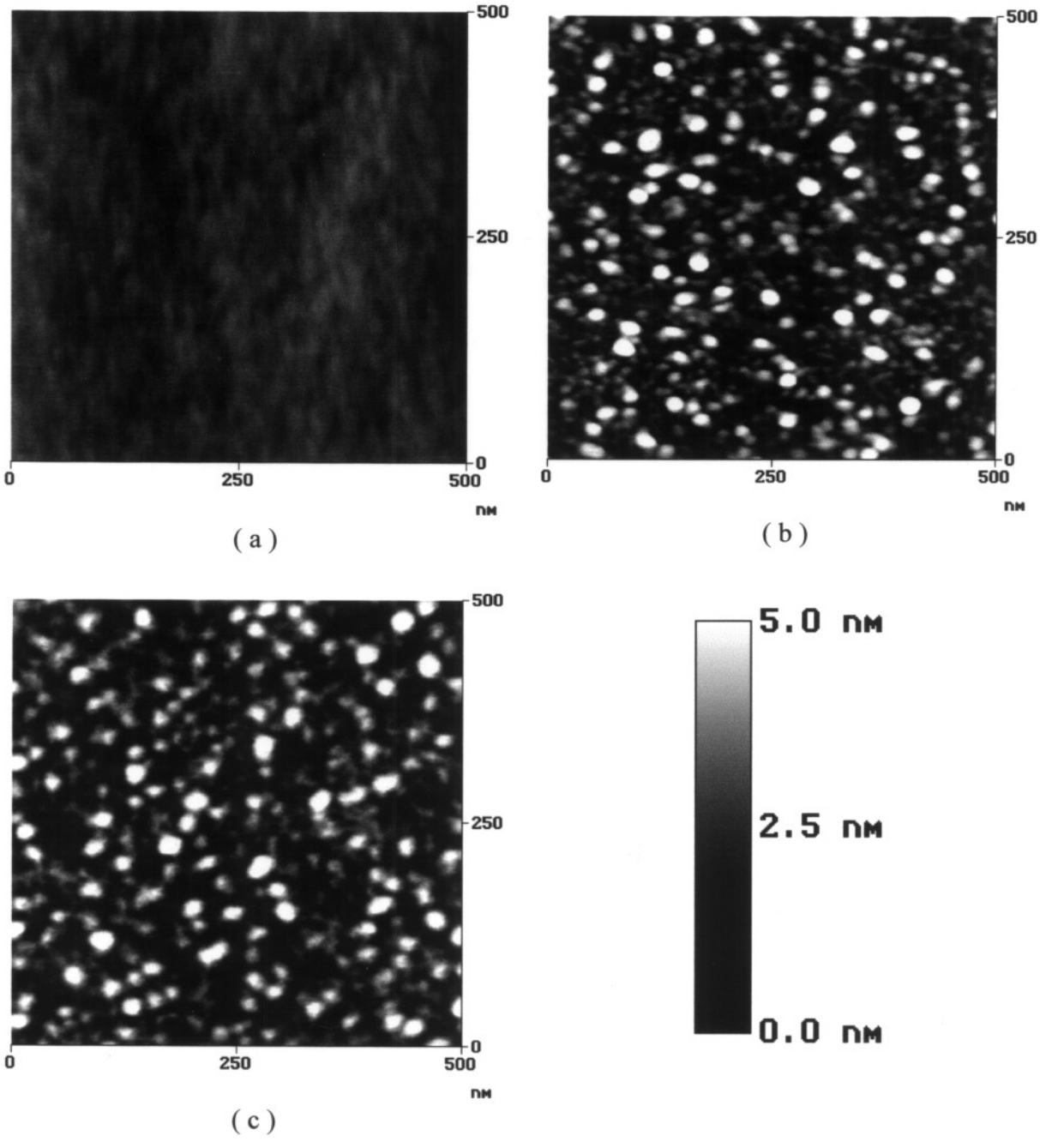

FIG. 3. TM-AFM images of the SiC(0001) surface and of samples #1 and #2: (a) 500 nm × 500 nm image of the SiC support; (b) 500 nm × 500 nm image of sample #1; (c) 500 nm × 500 nm image of sample #2.

of nine nearby atomic layers, deduced from the direct measurements by AFM.

In the case of sample #2 and sample #3 the number of particles increases significantly.

For sample #2, the surface coverage by Pd particles is estimated to 5.3%, with a mean diameter equal to 10.4 nm (Table 3). This reasonably agrees with a mean height value of 2 nm, as measured.

For sample #3 the density of Pd particles is too high, yielding distances between particles much smaller than the tip dimension which makes estimation of the particle number and size practically irrelevant. In any case, AFM measurements indicate clearly that there are no big Pd particles even for 2–6 Pd monolayers. A scenario in which Pd particles keep a rather constant (7–9 layers) height, but whose number first increases from low Pd content up to form a

TABLE 3

Number of Particles, Mean Diameter, and Height Calculated from the AFM Image of Fig. 3

	Number of particles (cm^{-2})	Diameter ϕ (nm)	Height h (nm)
#1 (1.9×10^{14} at/cm^2)	4.9×10^{10}	9.1 (3.50)	2.0 (0.62)
#2 (5.4×10^{14} at/cm^2)	6.2×10^{10}	10.4 (4.20)	2.0 (0.72)

Note. The number of Pd atoms and of Pd surface atoms is calculated for cylindrical particles. Standard deviation in parentheses.

quasi continuous film at 6 monolayer coverage, agrees well with the results.

In conclusion, the very thin palladium film can be regarded as formed by particles in the shape of disks of roughly 10-nm diameter and 2-nm height. The number of particles and their mean diameter increase with coverage, without important change of their height. As mentioned above the quantitative values given in Table 3 must be regarded as indications, rather than exact values.

The presence of relatively flat particles, clearly evidenced on samples #1 and #2, explains why the layer by layer approach we used fits well the XPS results. However, the height of these particles corresponding to something like 9 atomic layers, is probably large enough to expect 3D-like properties to the Pd particles, even for samples containing low quantities of metal. It is therefore surprising to measure quite high energy values for the $Pd_{3d5/2}$ binding energy, and one has to consider that some interaction between the Pd particles and the support does exist. Such an interaction could appear through direct chemical interaction or via some epitaxial strain effect. In any case, one has to think that such an interaction is retained even if the Pd coverage is increased, in the limit of the Pd coverages investigated, since the $Pd_{3d5/2}$ energy value does not change significantly with the Pd coverage.

Catalytic Reactivity of the Pd Deposits

The hydrogenation reactions were performed at T = 300 K, under a total pressure of about 20 mbar; the $P_{H_2}/P_{C_4H_6}$ ratio was 5. Runs performed on the clean support allow us to verify that the conversion of butadiene is negligible without deposited Pd.

A typical evolution of the butadiene, butenes, and butane pressures, monitored by mass spectrometry versus reaction time, is given in Fig. 4a. It corresponds to the data gained for the #3 sample. The conversion of butadiene to butenes is highly selective up to the total conversion of the butadiene. The linear decrease of the butadiene pressure versus time agrees with a zero order with respect to this reagent, which is generally observed (19).

The butadiene, 1-butene, cis-2-butene, trans-2-butene, and butane percentages monitored by gas chromatography are plotted against the reaction time in Fig. 4b. One can distinguish different phases during the hydrogenation reaction. First, 1-butene and trans-2-butene are mainly formed. Then, either just before the complete conversion of butadiene or at the beginning of butenes hydrogenation, a rapid isomerisation reaction is evidenced:

$$\text{1-butene} \rightarrow \text{2-trans-butene} + \text{2-cis-butene}.$$

The final phase corresponds to the hydrogenation of butenes. The 1-butene hydrogenation appears to proceed faster than that of 2-butenes, but it competes with the isomerisation reaction into 2-butenes. Such phenomena are commonly encountered in the case of pure Pd (20, 21). The combination of such a competition with different hydrogenation rates for 1- and 2-butenes, together with the significant decrease of the H_2 pressure in the course of the run, explains the nonlinearity of the curves reported in Figs. 4a and 4b after the total conversion of 1,3-butadiene.

To summarise, after the complete conversion of butadiene, the 1-butene is very rapidly isomerised to cis-butene and trans-butene, or converted to butane.

The reactivity diagrams of all the studied samples are quite similar in shape; only the time scale is changed. The catalytic activities for the butadiene → butenes conversion, deduced from these reactivity diagrams, are reported in Table 4. They are calculated for $P_{H_2} = 13.33$ mbar and with the assumption of a first-order reaction for H_2 as generally admitted (19). They are compared with the results previously obtained for pure Pd(111) and Pd(110) single crystals (22). One has to note that, in the case of Pd single crystals, the H_2 pressure was maintained at 6.67 mbar in order to avoid the bulk hydride formation which provokes the destruction of the monocrystalline state of the crystals. In the case of sample #1, assuming a 2-nm thickness for the Pd particles, as measured by TM-AFM, one has to consider that the reactivities measured per Pd surface atom of the

TABLE 4

1,3-Butadiene Hydrogenation Activities (Extrapolated for 13.33 mbar Hydrogen Pressure)

	#1	#2	#3	Pd (110)	Pd (111)
n^{Pd} (10^{15} atoms/cm^2)	0.19	0.54	2.9	0.94	1.54
Activity (10^{15} mol · cm^{-2} · s^{-1})	0.35	0.31	1.45	2.14	0.43
(mol · s^{-1} per Pd atom)	1.8	0.6	0.5		
(mol · s^{-1} per surface[a] Pd atom)	9[a]	3[a]		2.3	0.4

Note. The results for Pd(110) et Pd(111) are given for comparison (14).

[a] Calculated assuming uniform metal particles in shape of disks, with diameter $\phi = 10$ nm and height $h = 2$ nm. With such values, ≈20% of the total number of Pd atoms contained in a metal particle are in contact with the gaseous phase.

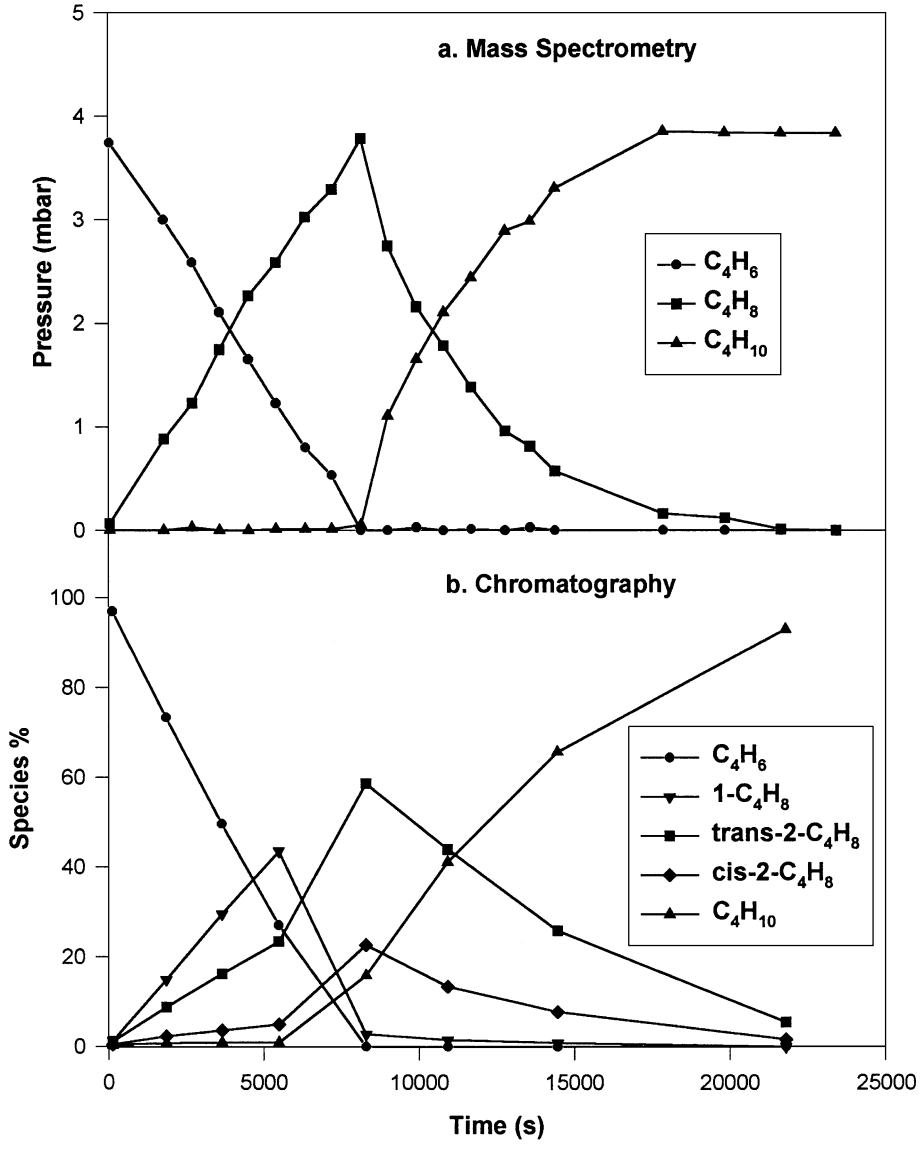

FIG. 4. Butadiene, butenes, and butane concentrations versus the reaction time as followed by (a) mass spectrometry; (b) gas phase chromatography. (Butadiene pressure = 3.8 mbar, hydrogen pressure = 19.2 mbar, deposit = 2.9×10^{15} Pd/cm^2.)

metal deposited on the SiC(0001) support are significantly higher than those measured per Pd surface atom of bulk materials. This phenomenon is similar for sample #2 while a bit less pronounced if one considers the values obtained for a given catalytic reaction and the morphology deduced from AFM. Since uncertainties in both catalytic and AFM measurements exist, the values calculated per Pd surface atom and reported in Table 4 have to be taken as tendencies rather than absolute values. In any case the reactivity of deposits are larger than those of pure Pd bulk materials. This can be attributed to some electronic effect induced by the support which would explain the higher value of the $Pd_{3d5/2}$ binding energy measured by XPS for the SiC-supported Pd particles, as compared to pure Pd. But, it is difficult to understand how this electronic effect could be still "visible" for these 10-nm diameter and 2-nm height, i.e. rather large, particles. Another effect which could increase the apparent reactivity of the Pd aggregates could be given, based on kinetics considerations, via a possible migration of some reactant impinging the support sufficiently near the metal particles, inside an extended area defined by the radius of capture, and migrating to the metal particles.

In Fig. 5 are reported the reactivity values we have obtained on different samples going from 1.9×10^{14} to 8.21×10^{15} Pd atoms/cm^2, most of them concentrated in our area of interest, i.e. between ~0.15 ML and ~2 ML Pd coverage. In a general way, the butadiene hydrogenation proceeds faster in the case of the more dense Pd deposits.

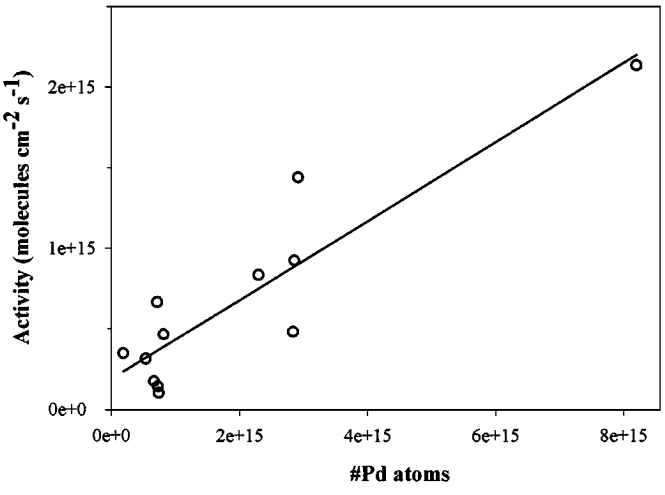

FIG. 5. Reactivity values obtained on different samples going from 1.9×10^{14} to 8.21×10^{15} Pd atoms/cm^2.

SUMMARY AND CONCLUSION

Thin layers of palladium (0.15 to 2 ML) obtained by atomic beam deposition of palladium on a C terminated SiC(0001) are constituted of relatively flat Pd aggregates. However, the particles formed are sufficiently high (around 9 atomic layers) to keep their metallic character. The number of Pd particles increases with Pd coverage, without noticeable increase of the particle size. Such a growth mode is quite different from that observed on supports like SiO_2, Al_2O_3, amorphous C, and HOPG graphite (6, 16–18) which exhibit a lot of surface defects acting as nuclei, and on which the number of particles is generally found to be quite constant; their sizes increase then with coverage and their-electronic and chemical properties are therefore changed. Unlike these supports, a growing process leading to the formation of rather large Pd particles takes place on the SiC(0001) substrate, even for low Pd content. The number of particles increase with the Pd coverage without significant modification of the physical properties.

The $Pd_{3d5/2}$ binding energy value of the Pd particles prepared by atomic beam deposition on SiC(0001) (more than 336 eV) is quite high, as compared to pure Pd (335.4 eV), or to Pd supported on cubic SiC catalysts prepared by chemical ways (334.8 eV) (24). This is an indication of some metal/support interaction which might depend on the way the SiC support was prepared and/or the metal was deposited onto the support.

The enhancement of the activity for the butadiene,1-3 hydrogenation reaction of the surface metal atoms of the Pd/SiC model catalysts so produced as compared to pure Pd could be due to some remaining interaction between the Pd particles and the SiC support, even if the metal particles appear to be quite large. In the limit of two-monolayer coverage, the activity of the "flat" Pd particles so produced remains proportional to the number of Pd atoms deposited.

REFERENCES

1. Vannice, M. A., Chao, Y. L., and Friedman, R. M., *Appl. Catal.* **20**, 91 (1986).
2. Ledoux, M. J., Hantzer, S., Cuong, P. H., Guille, J., and Desaneaux, M. P., *J. Catal.* **114**, 176 (1988).
3. Cuong, P. H., Marin, S., Ledoux, M. J., Weibel, M., Ehret, G., Benaissa, M., Peschiera, E., and Guille, J., *Appl. Catal. B, Environ.* **4**, 45 (1994).
4. Lednor, P. W., *Catal. Today* **15**, 243 (1992).
5. Boutonnet Kizling, M., Stenius, P., Anderson, S., and Frestad, A., *Appl. Catal. B, Environ.* **1**, 149 (1992).
6. Tardy, B., Noupa, C., Leclerc, C., Bertolini, J. C., Hoareau, A., Treilleux, M., Faure, J. P., and Nihoul, G., *J. Catal.* **129**, 1 (1991).
7. Nelder, J. A., and Mead, R., *Comput. J.* **7**, 306 (1965).
8. Zhong, Q., Inniss, D., Kjoller, K., and Elings, V. B., *Surf. Sci: Lett.* **290**, 688 (1993).
9. Lee, W. Y., *J. Appl. Phys.* **51**(6), 3365 (1980).
10. Zehringer, R., and Hauert, R., *Surf. Sci.* **262**, 21 (1992).
11. Muehlhoff, L., Choyke, W. J., Bozack, M. J., and Yates. J. T., Jr., *J. Appl. Phys.* **60**(8), 2842 (1986).
12. Parrill, T. M., and Chang Y. W., *Surf. Sci.* **243**, 96 (1991).
13. van Bommel, A. J., Crombeen, J. E., and van Tooren, A., *Surf. Sci.* **48**, 463 (1975).
14. Chang C. S., Tsong, L. S. T., Wang, Y. C., and Davies, R. F., *Surf. Sci.* **256**, 354 (1991).
15. Johansson, L., Owman, F., and Martensson, P., *Phys. Rev. B* **53**(13), 793 (1996).
16. Kohiki, S., *Surf. Sci.* **25**, 81 (1986).
17. De Gouveia, V., Bellamy, B., HadjRomdhane, Y., Masson, A., and Che, M., *Z. Phys. D, Atoms Mol. Clusters* **12**, 587 (1989).
18. Bertolini, J. C., Delichere, P., Khanra, B. C., Massardier, J., Noupa, C., and Tardy, B., *Catal. Lett.* **6**, 215 (1990).
19. Massardier, J., Borgna, A., Ouchaib, T., Moraweck, B., and Renouprez, A., *in* "Simposio Ibero-Americano de Catalyse, Trabalhos Tecnicos (Comissao de Catalyse Ed.) Petrobas, IBP **1**, 1990," pp. 529–538.
20. Bond, G. C., *in* "Catalysis by Metals," Academic Press, London, 1962.
21. Goetz, J., Ph.D. thesis, Université L. Pasteur de Strasbourg, 1995.
22. Massardier, J., Bertolini, J. C., and Renouprez, A., *in* "Proc. 9th Int. Congr. on Catal., Calgary **3**, 1988," p. 1222.
23. Mason, M. G., *Phys. Rev. B* **27**, 748 (1983).
24. Methivier, C., Beguin, B., Brun, M., Massardier, J., and Bertolini, J. C., *J. Catal.* **173**, 374 (1998).